Structural upgrade in three adjacent 6 MV linac bunkers operating simultaneously to limit exposure to radiation in controlled and uncontrolled areas

A. K. Vargas-Ramírez[a], E. Torres-García[a], J. Ramírez-Franco[b], J. O. Hernández-Oviedo[c], and A. V. Mercado-Quintero[d]

[a]*Facultad de Medicina, Universidad Autónoma del Estado de México,*
Paseo Tollocan s/n esquina Jesús Carranza, Colonia Moderna de la Cruz, C.P. 50180, Toluca, Estado de México, México,
e-mails: avargasr013@alumno.uaemex.mx; etorresg@uaemex.mx
[b]*Hospital San Javier,*
Av. Pablo Casals no. 640, Colonia Prados Providencia, C.P. 44670, Guadalajara, Jalisco.
e-mail: jramirezf@hospitalsanjavier.com
[c]*Centro de Cáncer ABC, The American British Cowdray Medical Center I.A.P. (CMABC),*
Calle Sur 136, no. 116, Colonia las Américas, 01120, Ciudad de México, México.
e-mail: omaovi@yahoo.com.mx
[d]*Department of Physics, University of York, Heslington, York YO10 5DD, United Kingdom.*

Received 23 August 2025; accepted 28 September 2025

The increasing in cancer incidence and advancements in teletherapy technology have necessitated shielding verification in linear accelerator bunkers, which may involve structural changes. This work proposes a hybrid methodology that combines analytical calculations and Monte Carlo simulation (TOPAS/Geant4 simulation toolkit) to determine, validate, and optimise shielding thicknesses in three adjacent bunkers where next-generation 6 MV linear accelerators will operate simultaneously. Findings indicate that the current secondary barriers in the hospital structure comply with international radiation exposure limits. However, the primary barriers require modifications to ensure radiological protection in both controlled and uncontrolled areas.

Keywords: Radiological protection; ionising radiation shielding; Monte Carlo simulation; teletherapy; ambient dose equivalent rate.

DOI: https://doi.org/10.31349/RevMexFis.72.021101

1. Introduction

Shielding of bunkers for clinical linear accelerators aims to maintain acceptable exposure levels in areas adjacent to the bunkers. These areas are classified as controlled zones, intended for occupationally exposed personnel (OEP) under radiological control, and uncontrolled zones, accessible to the public without radiological control. The ambient dose equivalent rate (ADER) limits for controlled and uncontrolled zones are 20 mSv/year and 1 mSv/year respectively. These criteria, established in NCRP Report No. 151, guide the structural design and shielding optimisation [1].

Shielding design in teletherapy rooms must adhere to strict standards in radiological protection [2–4]. However, achieving these levels is challenging in facilities with adjacent bunkers. Factors such as the simultaneous operation of linacs, beam overlap, gantry angular orientation, and the geometric arrangement of barriers increase the complexity of the design. These factors must be carefully considered to ensure radiological safety for both occupationally exposed personnel (OEP) and the public [5]. Additionally, over time, linacs are modernised, leading to changes in their X-ray spectra. This technological evolution necessitates shielding upgrades in bunkers that previously housed older equipment, in order to continue ensuring recommended radiological protection standards.

For the structural modernisation of linac bunkers, exposure levels must be evaluated [6]. If these standards are not met, one must model the facility geometry, the X-ray spectrum of the new equipment, and the interaction of radiation with shielding materials [7]. In this context, analytical calculations and Monte Carlo simulation (MCS) are essential tools to achieve such structural modernisation [8].

On one hand, analytical calculations are based on mathematical models established in international guidelines and recommendations, such as ICRP Publication No. 60 and NCRP Reports No. 151 and 49, which provide formulas and methodologies to estimate the required shielding thicknesses based on parameters such as workload, use factor, occupancy factor, and distance [1, 9, 10]. On the other hand, MCS, by generating virtual particles and statistically tracking their trajectories, allows for the estimation of equivalent dose distributions while accounting for multiple physical and geometric variables [11]. Previous studies [8, 12] have demonstrated the effectiveness of this approach in optimising shielding designs and reducing costs, while still ensuring compliance with regulations.

Specifically, TOPAS is the Geant4 simulation toolkit [13, 14], developed to facilitate advanced MCS for medical physicists across all forms of radiotherapy. This tool allows for modeling of X-ray treatment heads, patient geometries based on CT images, scoring of ambient dose equivalent, fluence, and more. It also enables saving and reproducing phase

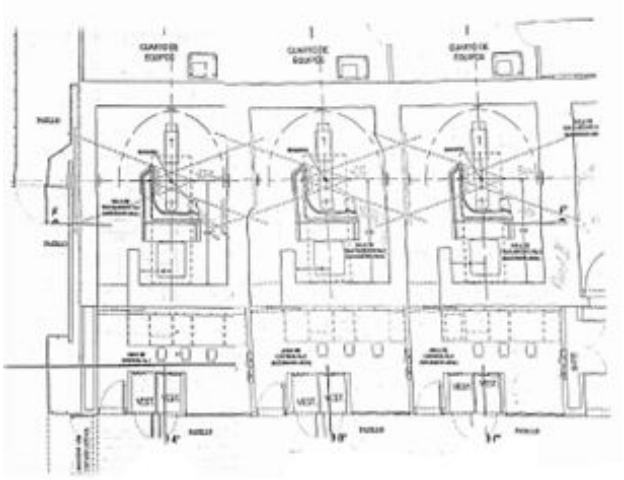

FIGURE 1. Original architectural plan of adjacent teletherapy bunkers at the Centro Médico Nacional Siglo XXI, Mexico City, Mexico.

space, provides advanced graphics, can determine barrier thicknesses in bunkers, among other key functionalities for shielding design.

Since the Centro Médico Siglo XXI-IMSS in Mexico City plans to replace three linacs, the structures of three adjacent bunkers that will house the new linacs must be updated. Therefore, the objective of this work is to use a methodology that combines analytical calculations and MCS (TOPAS toolkit) to determine the thicknesses of the primary and secondary barriers of these, where 6 MV linacs will operate simultaneously, such that the ADER in controlled and uncontrolled areas complies with national and international standards.

2. Metodologhy

The shielding design was carried out using two approaches: a) Manual thickness calculations based on the recommendations of NCRP Report No. 151 [1], and b) Monte Carlo simulation [11] using the Open-TOPAS toolkit version 4 [14].

The structure of the three adjacent bunkers is shown in Fig. 1; each bunker will house a 6 MV linac (Elekta, Infinity model).

2.1. Manual shielding calculation

Manual or analytical calculation allows determination of the required shielding thicknesses for primary and secondary barriers based on the established ADER limits at points or volumes of interest within controlled and uncontrolled zones.

The design was developed based on the technical specifications of the linac, including beam energy (6 MV), maximum radiation field size (40 $\times$ 40 cm), full gantry rotation (360°), and a leakage radiation of 0.1% of the primary beam. The total estimated weekly workload was also taken as 50,000 cGy/week, based on 45 patients per day over five

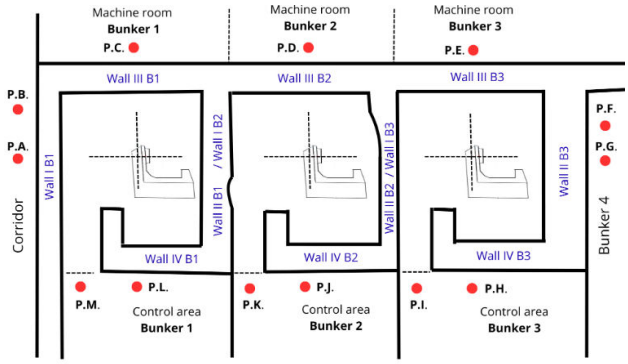

FIGURE 2. Identification of the different walls in the structure, points of interest, and boundaries of the three adjacent bunkers.

days a week, with an average dose of 2 Gy per patient, plus an additional 50 Gy/week for safety purposes related to quality control and dosimetry procedures [15].

Figure 2 shows the numbering of the teletherapy room walls used for the manual shielding thickness calculations, as well as the location of the points of interest labeled P.A., P.B., ..., P.R. Adjacent areas around the bunkers are also shown, with machine rooms and the corridor classified as uncontrolled zones, while the remaining areas are controlled zones.

The structure that forms the shielding and receives primary radiation from the source is referred to as the primary barrier, while the one that receives scattered or leakage radiation from the linac head is known as the secondary barrier [1].

The required thickness (t) of each wall needed to meet the ADER limit at the points of interest was calculated based on the tenth-value layer (TVL), as described below.

FIRST: The transmission factor B_x was obtained for the primary barrier; the secondary barrier, the factors for leakage radiation B_L and scattered radiation $B_{\rm PS}$ were calculated using Eqs. (1), (2) and (3), respectively.

$$B_X = \frac{P(dpri)^2}{WUT}, \tag{1}$$

where P is the weekly ADER limit beyond the barrier $(\text{Sv} \cdot \text{week}^{-1})$. $d_{\rm pri}$ is the distance from the X-ray target to the point of interest outside the bunker. W is the workload $(\text{Gy} \cdot \text{week}^{-1})$, measured at 1 meter from the X-ray target (isocenter). U is the use factor, with a value of 0.25 for primary barriers and 1 for secondary barriers. T corresponds to the occupancy factor, which depends on the adjacent area: for areas occupied full-time, such as treatment control areas, $T = 1$; for treatment rooms, it is $1/2$; for corridors, $1/5$; for treatment room doors, $1/8$; and for machine rooms, $1/20$.

$$B_L = \frac{1000P(d_{\rm sec})^2}{WT}, \tag{2}$$

where $d_{\rm sec}$ is the distance from the radiation source to the patient.

$$B_{\rm PS} = \frac{P(d_{\rm sca})^2(d_{\rm sec})^2 \cdot 400}{\alpha WTF}, \tag{3}$$

where d_{sca} is the distance from the isocenter or patient to the point of interest. F is the area of the incident field on the patient; α is the scatter fraction.

SECOND: Using Eq. (4) and applying only one value: B_x, B_L, or B_{PS}, depending on the case, the number of tenth value layers (n) required for each wall was determined.

$$n = \log\left(\frac{1}{B_X \cdot B_L \cdot B_{PS}}\right). \quad (4)$$

THIRD: Using Eq. (5), the required thickness for each barrier was obtained to ensure compliance with the ADER limit.

$$t(B_x, BL, B_{ps}) = TVL_1(B_x, BL, B_{ps}) + (n-1)\cdot TVL(B_x, BL, B_{ps}). \quad (5)$$

For secondary barriers, the two-source rule was followed [15]. The TVL values were taken from NCRP Report No. 151 for different barrier materials and beam energies, based on structural conditions and attenuation requirements.

2.2. Shielding verification and optimisation using Monte Carlo simulation

The effectiveness of the wall thickness obtained in the previous section in meeting ADER limits in the areas of interest was verified and optimised using MCS. The entire MCS process described below was also performed using the current wall thicknesses of the bunker, to assess the extent to which ADER limits are exceeded.

The MCS was carried out using the TOPAS/Geant4 simulation toolkit on a PC with a 4-core processor at 2.6 GHz and 8 GB of RAM. The three-dimensional structure of the adjacent bunkers was simulated based on the layout in Fig. 2. A cubic air volume of $14 \times 7 \times 30$ m was used as the logical world [16]. Within this space, geometric components were positioned, including: cylindrical phantoms with a radius of 20 cm and a height of 100 cm (visualized as blue circles), detectors with dimensions of $30 \times 30 \times 1$ cm^3 placed 30 cm from the walls and 50 cm from the floor and ceiling, corresponding to points P.A. through P.R. from Fig. 2 (red rectangles), and primary and secondary barriers (gray rectangles), as illustrated in Fig. 3. The shielding materials used were concrete, steel, and lead, defined according to the NIST database [17].

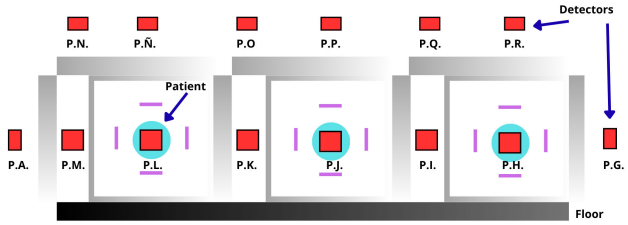

FIGURE 3. Simplified schematic of the geometry of components and subcomponents simulating the bunkers.

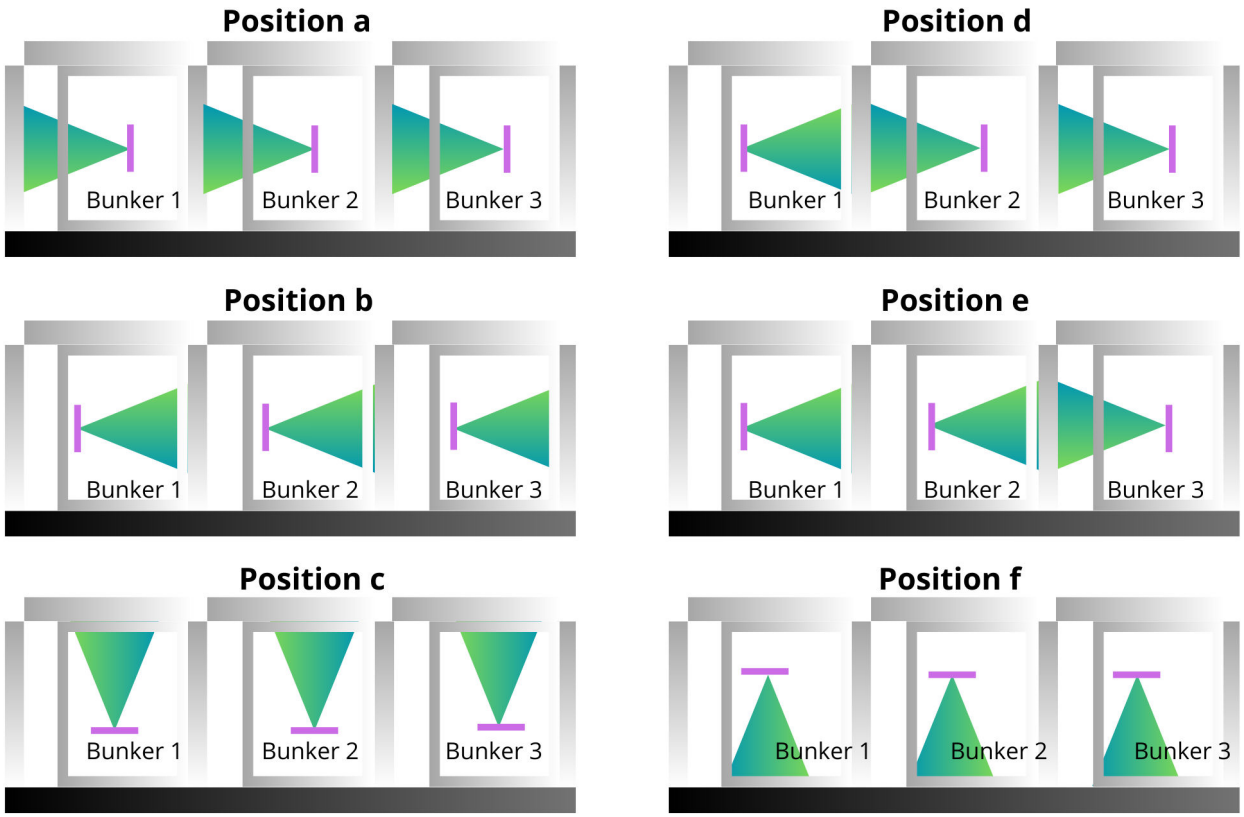

FIGURE 4. Gantry positions with the linac primary beam shown in green-blue. View in the Y-Z plane, where X represents depth.

The X-ray source for each simulated linac was obtained from a phase-space file in an International Atomic Energy Agency (IAEA) database, corresponding to a 6 MV ELEKTA Precise accelerator [18], whose characteristics are similar to the Infinity model.

In each simulation, all three linacs were operated simultaneously. The directions of the three beams were changed six times, as shown in Fig. 4. For each case, three runs were performed, each with 2×10^8 histories.

The simulation yielded the Ambient Dose Equivalent (ADE) per photon [19] in [mSv/photon] at the detectors (D_{det}) located at those positions, and at the patient phantom (D_{pac}) shown in Fig. 3. The fraction of ADE at the detector per unit dose delivered to the phantom was then obtained using the following ratio:

$$\frac{D_{\text{det}}}{D_{\text{pac}}}. \tag{6}$$

Considering that one working year equals 50 weeks, and that the workload (W) is 500 Gy/week (in this case, 1 Gy $=$ 1 Sv), and that T represents the occupancy factor, the annual ADE at the detector was obtained using the following Eq. (7):

$$ADE_{\text{annual}} = \frac{D_{\text{det}}}{D_{\text{pac}}} \cdot W \cdot 50 \cdot T. \tag{7}$$

The resulting annual ADE was then compared with the ADER limit. If the limit was exceeded at any of the detectors, the simulation was adjusted by increasing the barrier thickness through the addition of tenth value layers until the established ADER limit was reached. This closed the shielding design-verification-optimisation cycle, ensuring proper radiological protection.

Statistical uncertainty was determined using Eq. (8), through the analysis of standard deviations and relative errors [20].

$$EE = \frac{(\frac{SD}{\sqrt{N}})}{F}, \tag{8}$$

where SD represents the standard deviation obtained from the MCS of the variable of interest (e.g., equivalent dose); N is the total number of simulated histories; and F corresponds to the average number of particles (primary and/or secondary photons) that reach the detector within a specific time or spatial interval.

3. Results and discussion

The manual calculation results are presented in Tables I to III for each bunker. These results show the additional concrete thickness required, if any, according to the analytical calculations as well as its equivalent in steel or lead needed to comply with the ADER limit.

Since the structure of the existing hospital bunkers will be modified, there are space constraints. Therefore, it is recommended to add steel or lead so that the wall thicknesses do not increase significantly, while still ensuring the required radiological protection.

On the other hand, the MCS allowed modelling the three-dimensional geometry of the bunkers, as shown in Fig. 5 and in a simplified form in Fig. 3. First, the current thickness was modeled, followed by the thickness obtained from the manual calculations shown in Tables I, II, and III.

TABLE I. Calculated shielding thicknesses of teletherapy room 1.

Barriers	Current thickness	Additional calculated thickness	Equivalent in steel and lead
		Wall I	
Primary barrier	71 cm of concrete	65 cm of concrete	20 cm of steel (belt width 4.1 m)
Secondary barrier	71 cm of concrete	42 cm of concrete	13 cm of steel
		Wall II	
Primary barrier	71 cm of concrete	38.6 cm of concrete	12 cm of steel (belt width 3.7 m)
Secondary barrier	71 cm of concrete	16.4 cm of concrete	5 cm of steel
		Wall III	
Secondary barrier	76 cm of concrete	29.6 cm of concrete	9 cm of steel
		Wall IV	
Secondary barrier	71 cm of concrete	Not required	Not required
		Wall V (Ceiling)	
Primary barrier	55 cm of concrete	114 cm of concrete	20 cm of lead (belt width 3.3 m)
Secondary barrier	55 cm of concrete	84 cm of concrete	14 cm of lead
		Wall VI	
Door	N/A	90 cm of concrete	17 cm of lead
		Wall VII	
Floor	Not required		

TABLE II. Calculated shielding thicknesses of teletherapy room 2.

Barriers	Current thickness	Additional calculated thickness	Equivalent in steel and lead
		Wall I	
Primary barrier	71 cm of concrete	15.8 cm of concrete	5 cm of steel (belt width 4.4 m)
Secondary barrier	71 cm of concrete	3.4 cm of concrete	1 cm of steel
		Wall II	
Primary barrier	71 cm of concrete	32 cm of concrete	10 cm of steel (belt width 3.7 m)
Secondary barrier	71 cm of concrete	16.4 cm of concrete	5 cm of steel
		Wall III	
Secondary barrier	76 cm of concrete	Not required	Not required
		Wall IV	
Secondary barrier	71 cm of concrete	14.16 cm of concrete	5 cm of steel
		Wall V (Ceiling)	
Primary barrier	55 cm of concrete	114 cm of concrete	20 cm of lead (belt width 3.3 m)
Secondary barrier	55 cm of concrete	53.64 cm of concrete	10 cm of lead
		Wall VI	
Door	N/A	90 cm of concrete	17 cm of lead
		Wall VII	
Floor	Not required		

TABLE III. Calculated shielding thicknesses of teletherapy room 3.

Barriers	Current thickness	Additional calculated thickness	Equivalent in steel and lead
		Wall I	
Primary barrier	71 cm of concrete	32 cm of concrete	10 cm of steel (belt width 4.3 m)
Primary barrier	71 cm of concrete	16.4 cm of concrete	5 cm of steel
		Wall II	
Secondary barrier	138 cm of concrete	Not required	Not required
Primary barrier	139 cm of concrete	Not required	Not required
		Wall III	
Secondary barrier	76 cm of concrete	Not required	Not required
		Wall IV	
Secondary barrier	71 cm of concrete	Not required	Not required
		Wall V (Ceiling)	
Primary barrier	55 cm of concrete	114 cm of concrete	20 cm of lead (belt width 3.3 m)
Secondary barrier	55 cm of concrete	84 cm of concrete	14 cm of lead
		Wall VI	
Secondary barrier	N/A	90 cm of concrete	17 cm of lead
		Wall VII	
Door	Not required		

As shown in Fig. 5, each bunker was modeled with a ceiling, walls, door, and floors. Additionally, some of the detectors placed at the points of interest from P.A. to P.R. are visible.

The results of the simulation using the current shielding thicknesses of the hospital structure show that, at the points of interest located above the bunkers and in Teletherapy Room 4 (see Fig. 2), the limits established by international standards-20 mSv/year for occupationally exposed personnel (OEP) and 1 mSv/year for the public-are exceeded. Therefore, the current bunker shielding is insufficient to meet modern operational demands, such as the use of IMRT techniques and the simultaneous operation of multiple machines. As a result, the shielding must be redesigned, with special attention to the primary barriers.

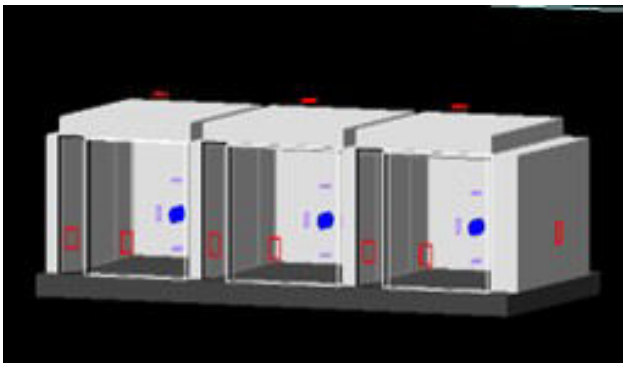

FIGURE 5. Three-dimensional geometry of the 3 adjacent bunkers simulated for primary barriers.

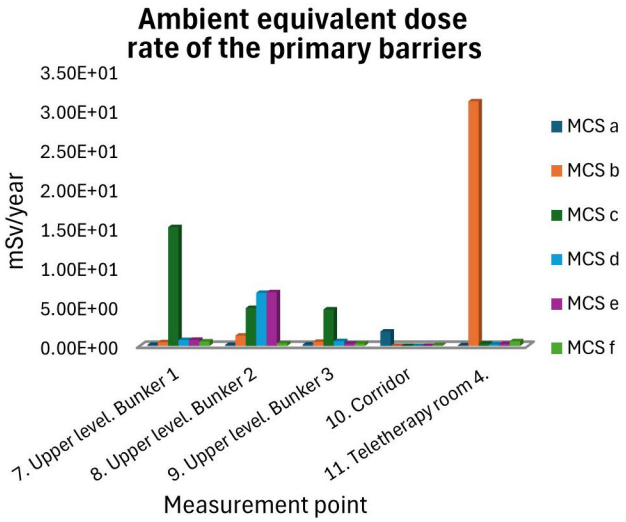

FIGURE 6. Equivalent dose rate resulting from the MCS using the manually calculated thicknesses (from the analytical report) for the primary barriers. Each zone includes 6 bars, and each colour represents the beam position shown in Fig. 4.

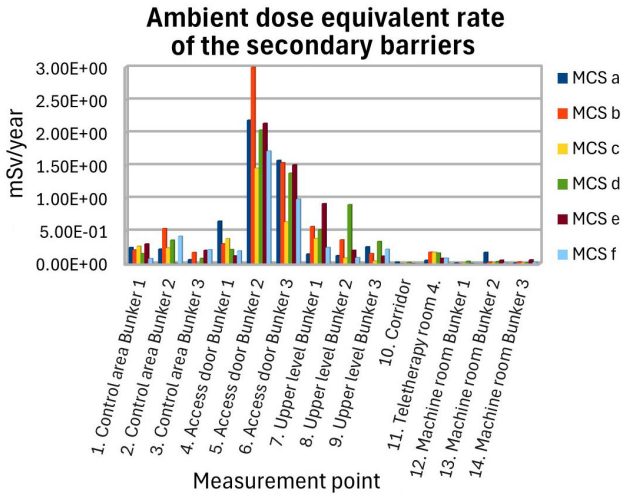

FIGURE 7. Equivalent dose rate from the MCS using the thicknesses calculated in the analytical report for the secondary barriers.

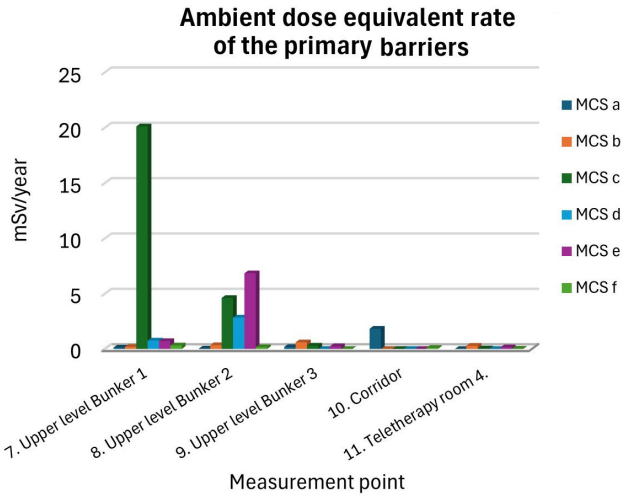

FIGURE 8. ADER from the MCS using the thicknesses modification of wall II of bunker 3.

Figures 6 and 7 show simulation results obtained using the manually calculated thicknesses from Tables I, II, and III. These results show that the calculated thicknesses of the secondary barriers comply with regulatory limits; in fact, the thicknesses appear to be overestimated, as the current thicknesses already meet the radiation protection requirements established by national and international standards.

However, one of the primary barriers-specifically Wall II of Bunker 3 (see Fig. 2)-requires an increase in thickness to meet the required radiation protection standards.

By increasing the thickness of Wall II of Bunker 3 by 0.301 TVL in the MCS to the manually calculated value (Fig. 8), the ADER complies with the limits established by international standards.

With this adjustment, the appropriate thicknesses are now in place for each of the primary and secondary barriers, ensuring compliance with international standards.

Regarding the statistical analysis of the simulations, the maximum uncertainty was around 25% in some detectors, with an average of 12.3% using 2×10^8 histories. Therefore, the number of histories was increased to 3×10^8, requiring a computation time of over one week for a single run; however, the uncertainty did not decrease significantly. Given the number of simulations required for this study, it was decided to proceed with 2×10^8 histories.

In this work, the shielding was calculated based on the specific workload information from the hospital in question (500 Gy/week for conventional radiotherapy with 45 patients per day). However, at present, treatments using hypofractionation regimens are being widely implemented; even so, the shielding thickness determined in the present work ensures that the exposure remains below internationally established levels. As hypofractionation regimens require more time per patient, only around 30 patients can be irradiated per day, resulting in a workload of around 430 Gy/week (considering 2.67 Gy in 15 fractions). The calculated shielding begins to

lose effectiveness when the number of patients treated per day exceeds 35.

4. Conclusions

The results show that no increase in the existing secondary barrier thicknesses is necessary to provide adequate radiation protection in both controlled and uncontrolled areas.

For the primary barriers, the analytically calculated additional thickness should be added to each barrier, which ensures adequate radiation protection for both occupationally exposed personnel (OEP) and the public. However, according to the MCS, one wall (wall II of bunker 3) requires an additional 0.301 TVL of concrete (or an equivalent material) on top of the analytically determined thickness to ensure radiation protection as established by national and international standards.

1. J. Deye, J. Rodgers, and R. Wu, NCRP Report No. 151: Structural Shielding Design and Evaluation for Megavoltage X and Gamma Ray Radiotherapy Facilities, https://www.severin.su/wp-content/uploads/2020/01/ncrp_151_structural_shielding.pdf (2005), ASM Press. Retrieved July 8, 2024.
2. Secretaría de Salud, Norma Oficial Mexicana NOM-002-SSA3-2017, Para la organización y funcionamiento de los servicios de radioterapia, *Diario Oficial de la Federación* (2017).
3. Secretaría de Salud, Norma Oficial Mexicana NOM-229-SSA1-2002. Salud ambiental, *Diario Oficial de la Federación* (2002).
4. Comisión Nacional de Seguridad Nuclear y Salvaguardias, Reglamento general de seguridad radiológica, *Diario Oficial de la Federación* (1988).
5. C. F. Arias, La regulación de la protección radiológica y la función de las autoridades de salud, *Revista Panamericana de Salud Pública* **20** (2006) 188.
6. G. Paredes, S. Genis, and B. Salazar, Determinación de niveles de radiación por neutrones en un acelerador para Radioterapia, *Congreso Nacional de Física Médica* (2018)
7. J. Gibbons, Khan's The Physics of Radiation Therapy, 6th ed. (Wolters Kluwer Health, 2020).
8. J. Rijken, S. Towns, and B. Healy, The need to update NCRP 151 data for 10 MV linear accelerator bunker shielding based on new measurements and Monte Carlo simulations, Journal of Radiological Protection **41** (2021), https://doi.org/10.1088/1361-6498/ac2e0b
9. R. Clarke *et al.*, Recommendations of the International Commission on Radiological Protection (1990).
10. National Council on Radiation Protection and Measurements, NCRP Report No. 49: Structural Shielding Design and Evaluation for Medical Use of X Rays and Gamma Rays of Energies up to 10 MeV (1990).
11. A. Bielajew, Fundamentals of the Monte Carlo Method for Neutral and Charged Particle Transport (The University of Michigan, 2020).
12. T. H. Sørensen, K. J. Olsen, and C. F. Behrens, Radiation protection of linac bunkers. A user-friendly approach, Radiation Protection Dosimetry **165** (2015) 503, https://doi.org/10.1093/rpd/ncv112
13. J. Perl *et al.*, TOPAS: An innovative proton Monte Carlo platform for research and clinical applications, Medical Physics **39** (2012) 6818, https://doi.org/10.1118/1.4758060
14. B. Faddegon *et al.*, The TOPAS tool for particle simulation, a Monte Carlo simulation tool for physics, biology and clinical research, Physica Medica **72** (2020) 114, https://doi.org/10.1016/j.ejmp.2020.03.019
15. J. Rodgers, Radiation therapy vault shielding calculational methods when IMRT and TBI procedures contribute, Journal of Applied Clinical Medical Physics **2** (2001) 157, https://doi.org/10.1120/jacmp.v2i3.2609
16. G. Collaboration, Book for application developers, vol. 10 (CERN, Geneva, 2019), pp. 5-2.
17. Geant4 Collaboration, Geant4 Material Database - Book for Application Developers. Version 11.3, https://geant4.web.cern.ch/documentation/dev/bfad_html/ForApplicationDevelopers/Appendix/materialNames.html (2024).
18. International Atomic Energy Agency, Phase-space database for external beam radiotherapy - Medical Physics: Radiotherapy, https://www.iaea.org/resources/hhc/medicalphysics/radiotherapy/equipment (2024), Retrieved June 11, 2024.
19. M. Pelliccioni, Overview of fluence to effective dose and fluence to ambient dose equivalent conversion coefficients for high energy radiation calculated using the FLUKA code, Radiation Protection Dosimetry **88** (2000) 279, https://doi.org/10.1093/oxfordjournals.rpd.a033046
20. A. V. Mercado-Quintero *et al.*, Novel photopeak-independent correction method for internal activity calculation of 99mTc: a simulation study, Radiation Protection Dosimetry **201** (2025) 105, https://doi.org/10.1093/rpd/ncae224